



MR Elastography of the Abdomen: Basic Concepts

Suraj D. Serai and Meng Yin

Abstract

Magnetic resonance elastography (MRE) is an emerging imaging modality that maps the elastic properties of tissue such as the shear modulus. It allows for noninvasive assessment of stiffness, which is a surrogate for fibrosis. MRE has been shown to accurately distinguish absent or low stage fibrosis from high stage fibrosis, primarily in the liver. Like other elasticity imaging modalities, it follows the general steps of elastography: (1) apply a known cyclic mechanical vibration to the tissue; (2) measure the internal tissue displacements caused by the mechanical wave using magnetic resonance phase encoding method; and (3) infer the mechanical properties from the measured mechanical response (displacement), by generating a simplified displacement map. The generated map is called an elastogram.

While the key interest of MRE has traditionally been in its application to liver, where in humans it is FDA approved and commercially available for clinical use to noninvasively assess degree of fibrosis, this is an area of active research and there are novel upcoming applications in brain, kidney, pancreas, spleen, heart, lungs, and so on. A detailed review of all the efforts is beyond the scope of this chapter, but a few specific examples are provided. Recent application of MRE for noninvasive evaluation of renal fibrosis has great potential for noninvasive assessment in patients with chronic kidney diseases. Development and applications of MRE in preclinical models is necessary primarily to validate the measurement against “gold-standard” invasive methods, to better understand physiology and pathophysiology, and to evaluate novel interventions. Application of MRE acquisitions in preclinical settings involves challenges in terms of available hardware, logistics, and data acquisition. This chapter will introduce the concepts of MRE and provide some illustrative applications.

This publication is based upon work from the COST Action PARENCHIMA, a community-driven network funded by the European Cooperation in Science and Technology (COST) program of the European Union, which aims to improve the reproducibility and standardization of renal MRI biomarkers. This introduction chapter is complemented by another separate chapter describing the experimental protocol and data analysis.

Key words Magnetic resonance elastography (MRE), Stiffness, Kidney, Preclinical imaging, MRI, Fibrosis

1 Introduction

Elastography based imaging techniques have received substantial attention in recent years for noninvasive assessment of tissue mechanical properties. These techniques take advantage of changed

soft tissue elasticity in various pathologies to yield qualitative and quantitative information that can be used for diagnostic purposes. Measurements are acquired in specialized imaging modes that can detect tissue stiffness in response to an applied mechanical force (compression or shear wave). Elasticity reflects the ability of tissue to deform and resume its normal shape under an applied stress and relates to tissue stiffness. Tissue stiffness in turn reflects tissue composition and structure. The primary desired output is to measure the level of stiffness. The measurement that helps differentiate if the tissue is hard or soft can give diagnostic information about the presence of the disease.

In the liver, tissue stiffness has been shown to be elevated with advanced fibrosis and to correlate with various stage of fibrosis [1–3]. Tissue stiffness can be estimated by imaging with either ultrasound (US) or magnetic resonance imaging (MRI). US-based elastography techniques include strain-based imaging, transient elastography (TE), and shear wave elastography (SWE). MRI measures tissue stiffness with magnetic resonance elastography (MRE). Other than strain-based imaging, which has largely been abandoned in the liver, all of these techniques (TE, SWE, and MRE) estimate tissue stiffness by measuring the speed of a shear wave traversing the tissue. In MRI, elastography encompasses imaging techniques that noninvasively estimate tissue elasticity and related mechanical properties through the application of external forces [4]. MRE is a phase contrast-based MRI technique for observing strain waves propagating in soft tissues (e.g., brain, heart, liver, spleen, breast, kidney, and muscle). Mechanical shear waves with frequencies of 40 to 200 Hz are induced using either a piezoelectric transducer or speaker coil oscillator directly coupled to the region of interest. By using multiple phase offsets and motion encoding gradients, MRE acquires data that allows the generation of images that depict shear wave motion and the calculation of local values of the tissue viscoelastic properties. In this chapter, we will provide an overview of MRE including the basic concepts involved, and a few illustrative applications of MRE in preclinical imaging.

This introduction chapter is complemented by a separate publication describing the experimental procedure and data analysis, which is part of this book.

This chapter is part of the book Pohlmann A, Niendorf T (eds) (2020) *Preclinical MRI of the Kidney—Methods and Protocols*. Springer, New York.

2 Measurement Concept

2.1 *Basic Concept of Stiffness Measured Using MRE*

MRE uses mechanical shear waves to evaluate the viscoelastic properties of tissues. In the abdomen, mechanical shear waves produced by an external driver are propagated into the tissue using an abdominal driver placed over the region of interest and in contact with the

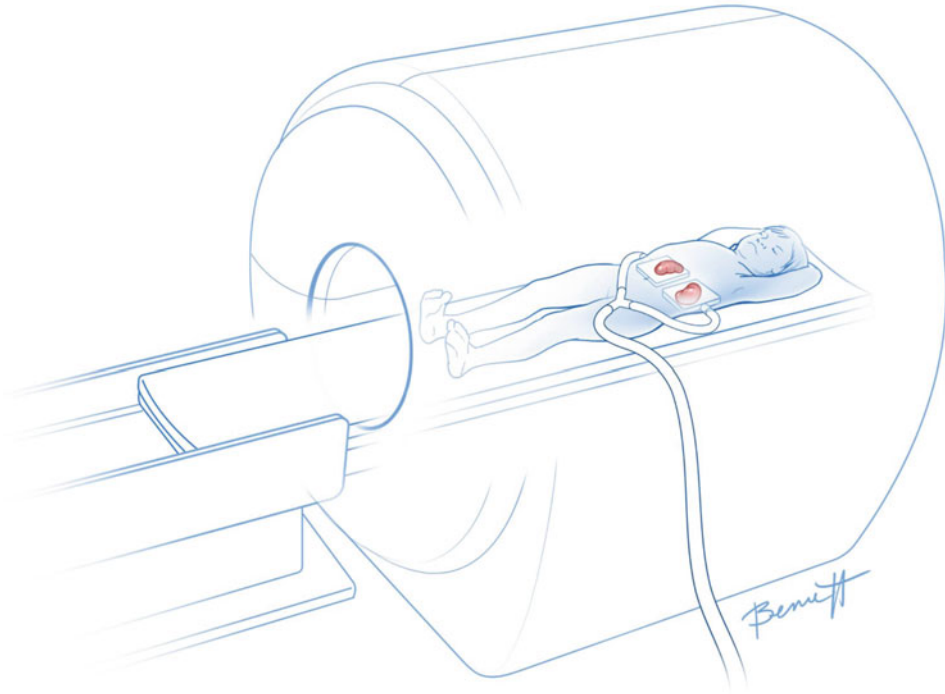


Fig. 1 Clinical MRE set up for the kidney

specific abdominal organ. Tissue displacements in the range of microns produced by propagating shear waves can be detected because phase shifts are encoded with motion encoding gradients in the MRE sequence. In liver, the typical frequency of shear waves used for clinical liver MRE is 60 Hz [5]. An accurate and reproducible stiffness measurement of organs such as pancreas and kidney, given their small size, complex geometry and boundary conditions, heterogeneous nature of the organ, and deeply seated location, requires 3D analysis of wave field data. For this reason, 3D MRE is recommended for such imaging. In 3D MRE, the propagating shear waves are imaged with a 2D multislice spin-echo echo-planar imaging (SE-EPI) pulse sequence modified to include the motion encoding gradients (MEG) in the X , Y , and Z directions. This is different from the 2D MRE typically utilized for liver imaging in which motion is encoded only in a single direction. An inversion algorithm automatically produces stiffness maps using the phase shift information. Shear stiffness values in kilopascals (kPa) are displayed for selected regions of interest in the target tissue. In renal MRE, the wave transmitting paddle is placed close to the kidney, preferably on the dorsal side (Fig. 1).

2.2 Generating Propagating Shear Waves

It is now well known that the MRE-measured shear modulus of soft tissue is dependent on the frequency of applied mechanical waves [6, 7]. That is why the term “shear stiffness” is often used to describe the shear modulus at a specific frequency. However, it should be fully understood that the formula that calculates the shear modulus from the measured velocity of the waves ($\mu = \rho c^2$, where μ = shear modulus, ρ = density of tissue, and c = wave speed) is valid only in purely elastic tissues.

In a typical MR elastography configuration, an active pneumatic mechanical wave driver is located outside the MR elastography room and is connected, by way of a flexible plastic (polyvinyl chloride) tube, to a passive driver that is fastened onto the abdominal wall or the abdominal organ or interest. The passive driver generates a continuous acoustic vibration that is transmitted through the abdomen, with a focus on the region of interest, at a fixed frequency, which typically lies in the range 40–400 Hz. A phase-contrast MRI pulse sequence with motion encoding gradients is synchronized to the frequency of mechanical waves created by the passive driver. This sequence is then used to image the micron-level cyclic displacements caused by the propagating shear waves to create a magnitude image, which provides anatomic information, and a phase difference image, which provides wave motion information. After the magnitude and phase images are created, an inversion algorithm can be used to process these raw data images to create several additional images and maps. The gray-scale elastogram is commonly used to provide quantitative stiffness measurement, in kiloPascals. The color elastogram is generally used for qualitative tissue stiffness evaluation. The color elastogram used clinically has a stiffness range of 0–8 kPa. A 0–20 kPa color elastogram is also created and is useful for appreciating tissue stiffness heterogeneity. For research purposes, the range can also be adjusted as desired. More details on image acquisition, postprocessing, and analysis are included in the chapter by Serai SD et al. “MR Elastography of the Abdomen: Experimental Protocols.”

2.3 Pulse Sequence for MRE Motion Encoding

The two types of acquisition sequences currently in use to obtain liver stiffness values are the gradient-recalled-echo (GRE) based (Fig. 2a) and the spin echo (SE) based with echo-planar readout (Fig. 2b); both of which have been shown to have excellent performance on both 1.5 and 3 T MRI scanners [8, 9]. The use of GRE-based sequence has been demonstrated to correlate with histological grading of liver fibrosis in previous studies and in a recent meta-analysis [8, 10]. The traditional GRE-based MRE acquisition works well on a 1.5 T scanner. However, the inherent limitations of GRE-based acquisition on field strengths at 3 T or higher are (1) enhanced sensitivity to susceptibility; T1 is longer at the higher field strength and hence signal drops off due to a longer echo time (TE); and (2) T2 and T2* are shorter at field strengths of 3 T and higher; hence, the relatively shorter T₂ and T₂* relaxation

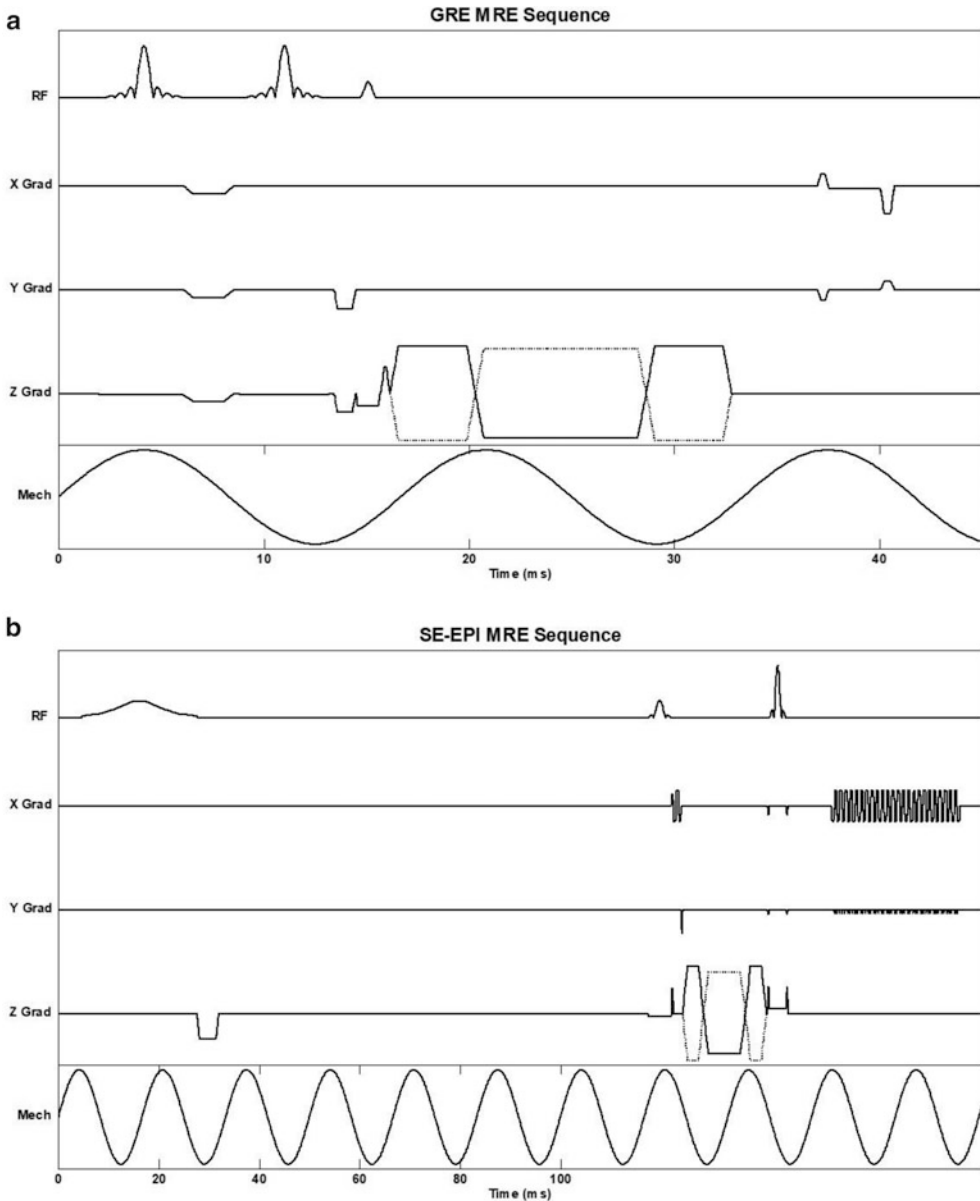


Fig. 2 (a) Pulse sequence diagram of a typical GRE-based MRE acquisition sequence and (b) SE-EPI-based MRE

time of the liver requires an even shorter TE. GRE-based MRE also has relatively lower accuracy in obese patients due to the increased distance from the driver to the liver. Thicker layers of fat can limit the acoustic penetration depth in the liver and produce limitations for encoding shear waves in the deeper areas of the liver, hence reducing the measurable area [9]. SE-EP-based acquisition overcomes this limitation by encoding more wavelengths per TR and hence can show more acoustic penetration. Since chronic liver

disease is quite frequently associated with obesity, radiologists should be aware of the limitations of GRE-based acquisitions in such cases. GRE-based MRE acquisition also requires relatively longer periods of acquisition and have a higher susceptibility to breathing motion artifacts. The current GRE-based protocol for MRE image acquisition requires a breath hold of approximately 20 s for a single slice. Echo-planar imaging (EPI), on the other hand, is a faster magnetic resonance imaging technique that obtains all spatial-encoding information in a single radiofrequency (RF) pulse, allowing shorter acquisition times with reduced motion artifacts. SE-EPI-based images are advantageous in patients with limited breath-holding capacity because they allow image acquisition of multiple slices within only one breath hold, and also enable measuring larger areas of the liver due to the greater number of waves encoded per relaxation time (TR). The drawback of SE-EPI-based acquisition is the potential increase in susceptibility artifacts due to an EPI-based readout. While technically more demanding, 3D-MRE offers advantages that might provide even higher diagnostic performance [11, 12].

3 Applications of MRE to the Abdomen

3.1 MRE for Evaluation of Liver Fibrosis

Liver fibrosis is an important pathological and pathogenic feature, and the assessment of fibrosis is often necessary for prognosis, risk stratification, clinical decision-making, and disease severity monitoring. Hepatic fibrosis eventually leads to cirrhosis, which is associated with a 50% 5-year mortality due to severe complications including variceal bleeding, hepatic failure, and development of hepatocarcinoma. Approximately 170 million people world-wide (3% of the global population) are infected with chronic hepatitis C (HCV), and 10–15% will develop cirrhosis within 20 years of infection [13]. Needle liver biopsy analyzed with connective tissue stains has long been considered the “gold standard” to detect and quantify hepatic fibrosis. Because of the cost, sampling variability, need for sedation, and risk associated with biopsy, noninvasive methods to assess liver fibrosis such as elastography are needed [14, 15]. MRE uses low-frequency (40–80 Hz) sound waves to induce shear waves in the liver, visualizes the shear waves by tracking tissue displacement using a modified phase-contrast sequence, and measures the speed of the propagating wave with specialized software called an inversion algorithm (Fig. 3) [16]. In Fig. 3, it can be seen that the red to blue region is a wavelength and this wavelength becomes longer in the presence of a stiff region for a given excitation frequency (Fig. 4). Then these wave images are converted into spatial stiffness maps (elastograms) using an inversion algorithm. Clinically MRE of the liver is FDA approved for human use and available on major MRI scanners. In the commercial version, the sound waves are generated by an acoustic subwoofer

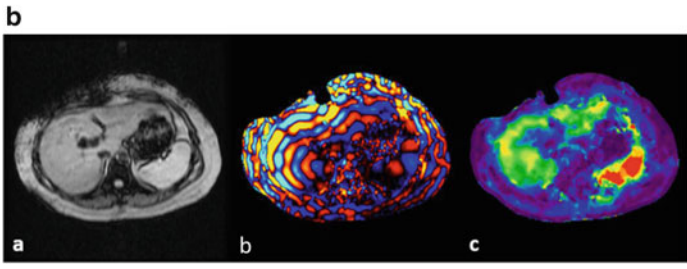
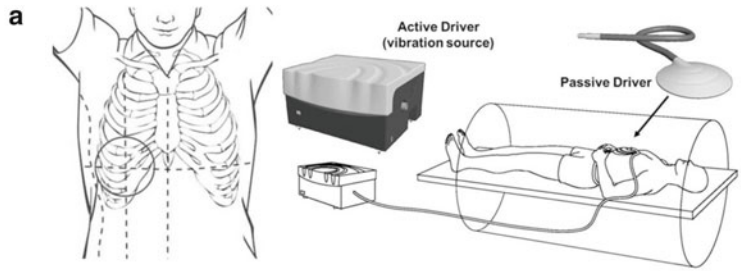


Fig. 3 Clinical MRE of the liver: **(A)** The passive driver should be placed over the right lower anterior chest wall at the level of the xiphisternum, centered on the mid-clavicular line. Once positioned, the passive driver should be held firmly against the chest wall by a wide elastic band, placed around the torso. Check to ensure that the band is stretched sufficiently so that the driver is not loose during full expiration. Note that the passive driver is connected via a plastic tube to the active driver (vibration source), which is located outside the scan room. **(B)** Magnitude and color-coded wave images of a successful MRE showing excellent illumination of waves through the liver. Stiffness map shows elevated liver stiffness consistent with significant fibrosis

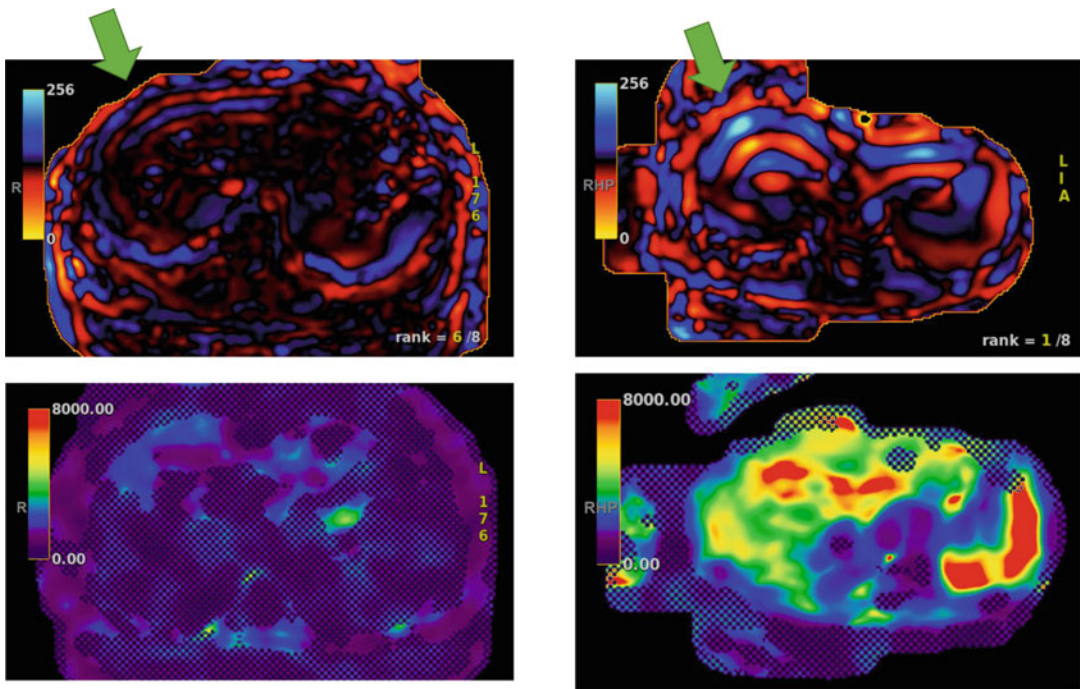


Fig. 4 Color (red and blue) wave images and its corresponding elastogram showing the difference in wavelength (green arrow) of a relatively “normal” subject vs. a patient with fibrosis

(called as “active driver”) outside the scan room and are transmitted to a plastic disk (called as “passive driver”) via a plastic tube passing through a wave guide [5]. During liver MRE image acquisition, the passive driver is secured by an elastic band over the right lower anterior chest wall. Most patients can feel the vibrations generated by the disk but do not find them uncomfortable. Identical MRE hardware and inversion algorithms are available on scanners manufactured by the three major MR vendors (GE, Philips, and Siemens) [10, 17]. MRE, as used clinically, currently has advantages over other tissue elastographic techniques. These advantages include the ability to further characterize tissue in terms of fat and iron content as well as standardization across manufacturer platforms, since the vast majority elastography hardware and software currently comes from a single manufacturer (Resoundant Inc.; Rochester, MN). Peer reviewed studies have shown that MRE is a robust, reliable, repeatable, and reproducible technique for detection and staging of liver fibrosis [10]. The accuracy of MRE has been reported to range from 0.85 to 0.99 for differentiating different stages of liver fibrosis [18]. The performance of MRE for differentiating mild fibrosis (stage 1) from normal liver or inflammation is lower and the performance is highest for diagnosis of cirrhosis (stage 4) [3, 10].

3.2 MRE for Evaluation of Liver Tumors

Motivated by the successful implementation of MRE for the study of diffuse changes in hepatic stiffness due to fibrosis, studies have been conducted to evaluate the potential role of MRE in characterizing hepatic tumors as malignant tumors appear to be stiffer than benign tumors [19–21]. In a preliminary work by Venkatesh et al., patients with 44 hepatic masses were evaluated with MRE and the results were correlated with pathological diagnosis or other accepted diagnostic criteria [20]. The stiffness of benign masses (nine hemangiomas, three focal nodular hyperplasia, and one hepatic adenoma) averaged 2.7 kPa, slightly higher than the mean stiffness of normal liver parenchyma (2.3 kPa). The mean stiffness of the malignant tumors was reported to be 10.1 kPa. The authors reported that a cutoff value of 5 kPa completely separated all benign liver masses from malignant lesions. Their results indicate that MRE shows substantial promise for aiding the characterization of liver tumors, which provides motivation for exploring the potential for evaluating other mass lesions in the abdomen as well.

3.3 MRE of the Spleen for Evaluation of Portal Hypertension

A study of 12 normal volunteers and 38 liver patients with biopsy-proven chronic liver diseases performed by Talwalkar et al., demonstrated higher spleen stiffness in patients with chronic liver disease and a very strong correlation between hepatic and splenic stiffness in these patients [22]. This may suggest that the bulk stiffness of the spleen is strongly affected by the portal venous pressure through a poroelasticity effect. A preclinical MRE study was performed on two adult mongrel dogs immediately after and 4 weeks

after initiating cholestatic liver disease by common bile duct ligation [23]. This preclinical model is known to have portal hypertension within 4 weeks. In this study subcutaneous vascular access ports were placed with catheter tips in the portal vein and the right hepatic vein allowing measurement of hepatic venous pressure gradient [23]. The MRE-assessed splenic stiffness in these dogs rose from a mean value of 1.8 kPa to an average of 3.4 kPa. The MRE study from the authors provide evidence to support the hypothesis that in the absence of confounding effects, the MRE-assessed stiffness of the spleen reflects the magnitude of the hepatic venous pressure gradient. This also provides motivation for the development of improved MRE techniques for the assessment of the spleen as well as the development and validation of poroelastic models that may allow the hepatic venous pressure gradient to be estimated noninvasively from MRE-based measurements of splenic stiffness. This would be a very significant development because knowledge of the hepatic venous pressure gradient is considered to be very important in the management of chronic liver disease and is very difficult to determine noninvasively. In a cross-sectional study of 25 patients with autosomal recessive polycystic kidney disease (ARPKD) and 25 healthy controls, ARFI based elastography was able to distinguish between participants without and with clinical signs of portal hypertension, namely splenomegaly or low platelets [24].

3.4 MRE of the Kidney

Many different disease mechanisms induce glomerular injury, including glomerulonephritis, hypertensive nephrosclerosis and diabetic nephropathy [25]. However, once renal damage reaches a certain threshold, progression of renal disease is consistent, and largely independent of the initial insult. This common pathway to end-stage renal failure is mainly due to tubulointerstitial damage characterized by tubular atrophy, loss of peritubular capillaries, and interstitial fibrosis. Mechanisms leading to kidney failure via tubulointerstitial damage and development of fibrosis are mostly massive proteinuria and chronic hypoxia [26]. Fibrosis further impairs oxygen diffusion and supply to tubular cells. This in turn exacerbates fibrosis of the kidney, rendering it into a vicious cycle.

Renal fibrosis is the excessive accumulation and deposition of extracellular matrix in the interstitial space of the kidneys. The process of fibrogenesis in kidneys is very complicated and cannot be attributed to any single type of cellular activity. However, it can be described as an overall result of the kidney's incapability to properly regenerate the damaged tissues after renal injury. When kidneys suffer injury, extracellular matrix deposition is an integral part of the damage repair process. However, certain processes can lead to excessive matrix to be deposited in the interstitial space, which leads to scarring of the kidneys. This interferes with the normal functioning of the kidneys and causes progressive loss of

renal function over time due to the reduction in the number of renal tubules. Renal fibrosis is a significant hallmark in the progression of CKD and can lead to end stage renal disease (ESRD), which necessitates dialysis or kidney transplant. Thus, in the assessment of chronic renal failure, fibrosis is a major histological feature and may be an important surrogate endpoint for prognosis and monitoring of treatment response. Besides, some investigations suggest that fibrosis might be reversible, when the cause is treated, emphasizing the need for early detection and quantification of this fibrosis [27–33]. Currently, renal biopsy is the gold standard for diagnosing kidney fibrosis. In this procedure, the kidneys of the patient are located with help of ultrasonography or X-rays. After determining the location, a needle is inserted in the kidney either percutaneously (called percutaneous biopsy) or after performing a cut near the region of kidney being observed under local anesthesia (called open biopsy) to obtain tissue samples [32, 33]. These samples are used for histological analysis to determine the presence of renal fibrosis.

Kidney biopsy has several limitations. It is invasive and causes pain to the patients after the procedure is performed. It is also associated with a prolonged hospital stay and higher costs and the procedure suffers from intra- and inter-observer variability. Since, only a small region from the entire kidney is used to obtain samples leading to potential sampling error [34]. Thus a noninvasive, truly quantitative method of interstitial renal fibrosis monitoring would be desirable. Diffusion-weighted and Blood Oxygenation Level Dependent (BOLD) MRI findings have been shown to be correlated to renal function [35–39], but no data has been published as to their correlation with the degree of fibrosis. Blood or urinary markers of fibrosis are also currently evaluated but neither is used in clinical practice yet [40].

MRI and ultrasound (US)-based methods can estimate tissue stiffness (and thus the degree of fibrosis) by measuring the velocity of shear waves traveling through the organ of interest [41, 42]. US-based elastography techniques are mainly classified under strain imaging (SI) or shear wave imaging (SWI). The basic principle of SI is application of stress to the tissue and measuring the resulting normal strain which is reported as Young's modulus. SWI-based techniques use either a dynamic vibrating device or acoustic radiation force to generate shear waves in the tissues, which are reported either as shear wave speed or Young's modulus. Techniques based on SI include strain elastography (SE) and acoustic radiation force impulse strain imaging (ARFI), whereas SWI-based techniques include point shear wave elastography (pSWE), 2D shear wave elastography (SWE), and 1D transient elastography (TE).

Studies have used both SI and SWI to investigate renal fibrosis. SI-based techniques are found to be beneficial for diagnosing renal

fibrosis in allografts than native kidneys [43]. This is because external compression can be efficiently applied to allografts located superficially than to native kidneys which are located retroperitoneally thereby limiting accuracy of this technique. A study by Menzilcioglu et al. reported that even though SE reported higher mean strain index in CKD patients when compared to healthy subjects, it could not differentiate between various stages of CKD [44].

SWI-based techniques have an advantage over SI-based techniques since they do not depend on external compression. However, studies using SWI have reported conflicting results. A study by Wang et al. reported that shear wave velocity measurements did not show any correlation with degree of renal fibrosis [45]. Few studies have reported lower shear wave velocities in patients with CKD than in healthy subjects [46]. It has been observed that there is a negative correlation between shear wave velocity and progression of CKD in kidneys whereas a positive correlation has been observed in liver using the same SWI-based techniques [43]. Apart from these conflicting results, US-based elastography techniques have following limitations: (1) only provides 1D or 2D stiffness of the kidneys; (2) requires extensive training of technicians and is still prone to inter- and intraobserver variability; (3) highly dependent on the body mass index of subjects; and (4) anisotropy of the kidney can impact the results. The US-based transient elastography (Fibroscan™ device) is able to discriminate the different stages of liver fibrosis with a quadratic trend of the curve plotting histologic scores versus elasticity measurements [47]. Among patients with cirrhosis, stiffness thresholds predicting the onset of specific complications (ascites, oesophageal bleeding, hepatocarcinoma, etc.) have been identified. However, as explained with the limitations of US based studies, this technique is limited by its 1D nature in that it does not allow the exploration of the entire liver. MRI has advantages over US since it can image organs located deep in the human body with good image contrast and spatial resolution thereby improving the diagnosis. It also does not involve use of any radiation and therefore can be used to monitor progression of diseases over a period of time. MRE has been successfully used to assess and stage liver fibrosis. The shear stiffness of normal liver was found to be approximately 2.2 kPa by several independent groups, using vibrating frequencies of 60 Hz [1, 3]. MRE has been shown to successfully discriminate the different stages of liver fibrosis, with the same quadratic trend of the fibrosis/elasticity curve and a recommended cut-off value derived from a large group of patients [18]. MRE has the advantage of being intrinsically a 2D technique and can be associated to conventional liver imaging at the same time. In the kidney, evaluation of interstitial fibrosis is crucial to the assessment of prognosis and to guide therapy for most kidney diseases. However, how best to measure kidney fibrosis remains

Cor 2D MRE

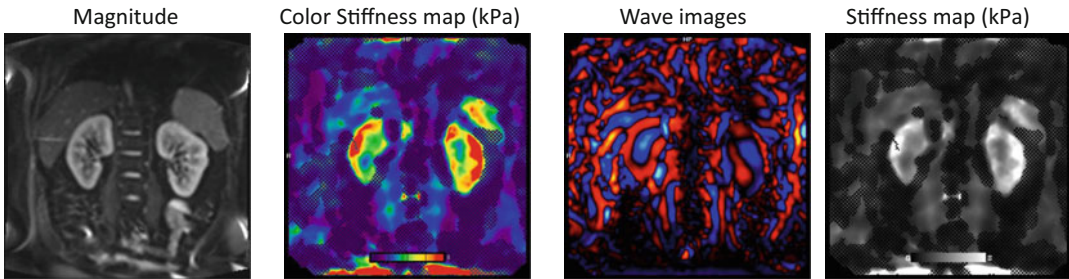
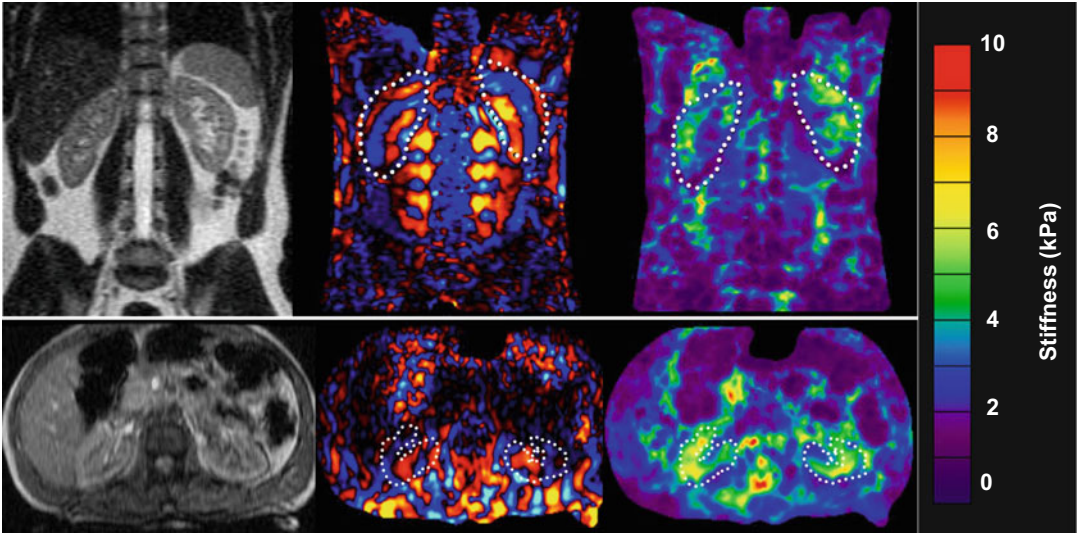


Fig. 5 MRE of the kidney of a healthy volunteer performed at 60 Hz. Magnitude, stiffness map and color-coded wave images of a successful MRE showing excellent illumination of waves through the kidney. The stiffness of the normal kidneys at 60 Hz ranged from 3.5 to 5 kPa

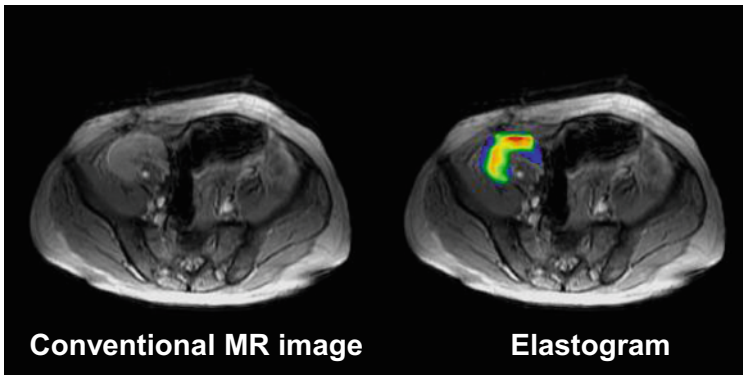
uncertain. An MRE-based technique that measures tissue stiffness, would be a novel application for assessment of renal fibrosis. The resulting microscopic vibrational waves passing through the organ generate shear waves that can be imaged with motion-synchronized MRI. The velocity of wave propagation is dependent on organ stiffness, with stiffer fibrotic tissue leading to more rapidly moving waves with longer wavelength. Exploratory MRE of the kidneys in healthy volunteers has demonstrated that shear waves can be readily generated and imaged in this organ. Unlike the liver and spleen, the patterns of wave propagation in these structures are extremely complex and include significant components propagating at oblique angles relative to an axial plane of section. Given these characteristics, it is necessary to image the pattern of wave propagation in three dimensions and to obtain data from all three polarizations of motion, which requires longer imaging times. This kind of 3D/3-axis MRE acquisition is problematic if the imaging is to be conducted during suspended respiration and using a GRE-based acquisition method. One approach to this is to use respiratory gating, though this can make the total acquisition times quite long. As an alternative, EPI-based techniques can be used to significantly reduce acquisition times. EPI-based MRE sequence have been shown to be capable of acquiring 12 wave images (four phase offsets at each of three motion-encoding directions) with an acquisition time of 8 s per slice. This technique has successfully generated 3D wave data sets with typical voxel dimensions of 4 mm (Figs. 5, 6, and 7). With a 3D extension of the inversion software, including 3D spatial filtering, the preliminary results indicate that it is quite feasible to image tissue stiffness throughout a larger 3D region of interest in the abdomen and has yielded provocative preliminary results in the kidneys that motivate further development in this organ.



MRE of kidneys performed in two normal healthy volunteers.

MRE performed in coronal and axial planes at 90Hz. The dotted lines on the wave images and stiffness maps outline the kidneys. The stiffness of the normal kidneys ranged from 5 to 7.5 kPa

Fig. 6 MRE performed in coronal and axial planes at 90 Hz. The dotted lines on the wave images and stiffness maps outline the kidneys. The stiffness of the normal kidneys at 90 Hz ranged from 5 to 7.5 kPa (Image courtesy of Dr. Sudhakar Venkatesh, Mayo Clinic, Rochester, Minnesota, USA)



MRE of renal graft in the right iliac fossa 4-months following transplantation.

Stiffness is similar to normal kidneys. The renal function was normal. Biopsy showed no interstitial fibrosis or tubular atrophy.

Fig. 7 MRE of renal graft in the right iliac fossa acquired 4-months following transplantation. Stiffness is similar to normal kidneys. The renal function was normal. Biopsy showed no interstitial fibrosis or tubular atrophy (Image courtesy of Dr. Sudhakar Venkatesh, Mayo Clinic, Rochester, Minnesota, USA)

Pilot studies of MRE have been performed in native kidneys and kidney allografts, attempting to correlate kidney stiffness with either fibrosis burden or kidney function [48]. Although MRE in porcine kidneys showed a correlation between stiffness and fibrosis in the medulla, the results of small pilot human studies have so far been conflicting, and no studies, as yet, have assessed whether stiffness measured by MRE predicts progression of kidney dysfunction [49]. MRE may also be helpful in the evaluation and follow-up of patients undergoing renal transplant [50]. In a study by Orlichio et al., real-time elastography was able to evaluate kidney fibrosis in a noninvasive way and could be used as complementary imaging during follow-up of renal transplant patients [51].

3.5 MRE of the Pancreas

Pancreatic fibrosis is often associated with chronic pancreatitis, pancreatic ductal cancer, or inflammatory pseudotumor [52]. Since pancreatic fibrosis may affect decisions of surgical interventions and prognosis in such pathologies [53], MRE techniques could be exploited for information concerning pancreatic fibrosis reflected by its stiffness. Serai et al. have demonstrated that 3D MRE of the pancreas is feasible in children with and without pancreatic disease, in a small cohort of pediatric patients, referred for clinical imaging with history of acute recurrent pancreatitis (APR) or CP [12]. In this preliminary study, they observed statistically significant lower pancreas stiffness values derived from 3D MRE in children with a history of ARP or CP as compared to healthy control children (1 kPa vs. 1.7 kPa) [12]. The finding of lower pancreas stiffness in ARP/CP than controls is contrary to the findings reported in a small series of adults (mean age 55.6 years) by An et al. [54]. In their study, a mean stiffness value of 1.1 kPa was reported for healthy controls compared to a mean stiffness of 1.5 kPa in five patients with chronic pancreatitis. Further, a study by Wang et al. reported mean stiffness values of 1.5 and 1.9 kPa in adults with mild ($n = 30$) and moderate to severe ($n = 16$) chronic pancreatitis respectively as classified by the Cambridge criteria [55]. Reported stiffness values in patients were higher than the values in healthy patients in the same study.

3.6 Other MRE Body Applications

Since MRE is a new, multistep MR technique, there is potential for improvement, expansion and exploration. Breast tumors are known to be stiffer than normal breast tissue and hence manual palpation is a recommended part of routine screening that helps in the detection of tumors [56]. MRE is being investigated in breast imaging for the detection of breast cancer since this disease is one of the leading causes of death in women and the current diagnostic methods are not satisfactory [57, 58]. Skeletal muscle MRE can be used for studying the physiological response of diseased and pathological muscles [59]. For instance, it has been found that there is a difference in the stiffness of muscles with and without neuromuscular

disease [60]. In a recent study on patients with Duchenne muscular dystrophy, the authors concluded that shear wave elastography could be considered a useful noninvasive tool to monitor muscle changes in early stages of the disease [61].

4 Influence of Perfusion on Abdominal Organs

Preliminary results from the studies relating splenic stiffness to hepatic venous pressure gradient (HVPG) suggests that the stiffness of abdominal organs may have two components: a static component reflecting intrinsic structural properties and a dynamic component reflecting extrinsic perfusion changes [62, 63]. To investigate the influence of perfusion on the shear stiffness of abdominal organs, studies of specific conditions of the liver and kidneys are being actively pursued [64].

4.1 Post-prandial Influence on Liver Stiffness

Food intake is known to cause an increase in mesenteric blood flow, which may lead to a postprandial increase in hepatic stiffness that is different in patients with hepatic fibrosis than in normal volunteers [65]. It has been observed that MRE-assessed liver stiffness increases significantly (average increment of 18% with ranges from 5% up to 48%) following a test meal in patients with advanced hepatic fibrosis, whereas fasting and postprandial liver stiffness are similar in the normal state [65]. This finding suggests that there is a dynamic component to the liver stiffness that is dependent on the portal pressure. Therefore, it is very important to have hepatic MRE examinations performed consistently in a fasting state. The postprandial augmentation in hepatic stiffness after a test meal known to increase mesenteric blood flow is likely due to the transiently increased portal pressure in patients with hepatic fibrosis. It is thought that mechanical distortion of the intrahepatic vasculature caused by fibrosis impairs the autoregulatory mechanism for the portal venous pressure, which may cause acceleration of the development of portal systemic varices and stretching of hepatic parenchyma and stellate cells that are instrumental in the progression of hepatic fibrosis. This promising observation provides motivation for further studies to determine the potential value of assessing postprandial hepatic stiffness augmentation for predicting progression of fibrotic disease and the development of portal varices. It may also provide new insights into the natural history and pathophysiology of chronic liver disease.

4.2 Influence of Hydration on Renal Stiffness

Stiffness plays an important role in diagnosing renal fibrosis. However, kidney stiffness is altered by perfusion changes in many kidney diseases. A study by Clark et al. suggests that increasing water intake is recommended for patients with CKD as it helps to preserve renal function [66]. Water intake before a MRE scan can act also as a confounding factor to estimate the stiffness of kidneys. In a recent

study, Gandhi et al. observed a negative correlation between difference in stiffness values and changes in bladder volumes before and after water intake [67]. This suggests that at lower bladder volume the kidneys are still filtering the water where perfusion pressure is high leading to an increased stiffness in the kidneys.

4.3 Stenotic Kidney MRE

The kidney is a richly perfused organ receiving 25% of the cardiac output. Renal occlusions, such as renal arterial stenosis, threaten the viability of the kidney by diminishing blood flow leading to irreversible tissue fibrosis and ultimately kidney failure. Preliminary research has been performed to study the impact of renal arterial stenosis on kidney stiffness in a porcine model of acute renal arterial stenosis [68]. MRE measurements showed that the stiffness of the kidney progressively decreased as the renal artery stenosis was increased. The authors reported that the stiffness of the contralateral kidney was observed to increase progressively, which indicates that hemodynamics can significantly affect the mechanical properties of renal parenchyma. Fibrosis is associated with elevated tissue stiffness. However, studies have indicated the rich perfusion of the kidney may affect its distension and, in turn, stiffness [68]. In order to determine the interdependent relationship between perfusion, fibrosis and stiffness, an acute renal arterial stenosis model was established in adult pigs by isolating the renal artery to insert a vascular occluder and an embedded Doppler flow probe. The renal blood flow (RBF) was gradually reduced from the baseline level to total occlusion of 100% with MRE acquisitions performed at each step. The cortex of the acutely stenotic kidney decreased in stiffness as the degree of stenosis was increased to 40% and above. The systemic blood pressure also rose during each decrement in the RBF (from 75 ± 3 to 96 ± 3 mmHg). These preliminary renal MRE results encourage the further evaluation of renal hemodynamics on tissue stiffness, which may be due, in part, to perfusion pressure applied to the organ. These factors may also play a complicating role in detecting the presence of fibrosis due to renal arterial stenosis, and hence may lead to new techniques to assess tissue stiffness. The use of MRE to assess changes in tissue mechanics associated with the dynamic perfusion of tissue may also provide new insights into the natural history and pathophysiology of renal diseases (Table 1).

5 Preclinical MRE

Increasing evidence has demonstrated that, unlike cirrhosis, the early stages of fibrosis are treatable and reversible if appropriate antifibrotic treatment is given [69, 70]. As antifibrotic therapies evolve, a reliable, noninvasive assessment of hepatic fibrosis is needed to manage patients with chronic liver disease. Being able

Table 1
Factors confounding the tissue stiffness measured using MRE

Confounding factor	Direction of effect	Examples scenarios
Iron/ T_2^*	Loss of SNR	Patients with B-Thalassemia
Inflammation	Positive	Patients with AIH
Congestion	Positive	Patients with Fontan
Magnetic-field (B_0) inhomogeneity	Positive	Bowel gas, poor shim
Steatosis/fat	Negative	Patients with NAFLD, NASH
Renal stenosis	Negative	Patients with renal artery stenosis or perfusion defects
Renal perfusion	Positive	Large hydration volume or higher renal perfusion pressure can alter renal stiffness

A “positive” direction of the effect means that an increase in the confounding factor leads to an increase in measured stiffness and hence an overestimation of the fibrosis, and a “negative” direction of the effect means that decreases the confounding factor lead to a potential under estimation of stiffness

to noninvasively monitor the progression of liver fibrosis helps in understanding the natural history of liver fibrosis in patients with chronic liver disease, determining which patients require antiviral therapy, predicting the approximate time to the development of cirrhosis, and discovering new directions of scientific inquiry. Similarly, being able to early diagnose renal fibrosis or parenchyma damage would help in understanding the natural history of renal fibrosis in patients with CKD, determining which patients require which therapy, predicting the approximate time to the development of renal failure, and discovering new directions of scientific inquiry. Therefore, there are ongoing investigations using preclinical models with a reliable, noninvasive method to assess fibrosis, not only to detect and stage the disease itself but also to monitor treatment efficacy and optimize dosing. In recent work by Yin et al. [2] feasibility of MRE was demonstrated on a mouse model of autosomal recessive polycystic kidney disease (ARPKD), which is an inherited disorder of the kidneys and liver caused by mutations in the PKHD1 gene and an important cause of congenital hepatic fibrosis (CHF) in humans. A renal wrapping surgery performed on eight pigs to induce systemic arterial hypertension, showed that MRE derived aortic stiffness increased with mean arterial pressure [71].

5.1 Considerations Regarding Animal Preparation

- Bowel gas can create susceptibility artifacts in renal imaging; right lateral position helps minimize susceptibility artifacts from bowel gas.
- Respiratory motion can create artifacts and if necessary free breathing methods may be needed to minimize them. Alternatively, respiratory triggering could be used, but this may increase the acquisition time [72].
- Studies indicate the choice of anesthesia may have an effect on quantitative MR measurements. This may be partly due to known effects of anesthesia on respiration, temperature, blood pressure, and pO₂.
- Hemodynamic variables may modulate kidney stiffness measured by MRE and may mask the presence of fibrosis [68].
- In liver imaging, elevated stiffness is observed “after meal” due to postprandial effect. Such effects have not yet been reported in measuring kidney stiffness [65].
- While performing renal MRE, renal perfusion status should be taken into account to ensure reproducible detection [73]. Confounding stiffness changes due to excess water intake have been reported [67].
- In the preclinical setting, motion artifacts can usually be minimized using multiple averages.

6 Conclusion

Renal fibrosis causes a change in the anatomy of kidneys wherein there is an excess accumulation of interstitial extracellular matrix and reduction in the number of tubules. Elasticity imaging is an imaging field that has received considerable attention due to its intuitive mechanical contrast based on “palpation” and its great diagnostic potential. Elasticity imaging techniques are based on measuring the response of tissues to an applied excitation and different approaches have been proposed and investigated toward this goal. Elastography encompasses imaging techniques that non-invasively estimate tissue elasticity and the related mechanical properties through the application of external forces. Elasticity reflects the ability of tissue to deform and resume its normal shape under an applied stress and relates to tissue stiffness. Tissue stiffness in turn reflects tissue composition and structure. Fibrosis is an important pathologic and pathogenic feature of each of these conditions, and the assessment of fibrosis is often necessary for prognosis, risk stratification, clinical decision-making, and disease severity monitoring. Due to the cost, need for sedation, and risk associated with biopsy, noninvasive methods such as elastography to assess tissue fibrosis are needed.

US-based methods only provide 1-D stiffness, have lower penetration depth and are highly dependent on body mass index, anisotropy of tissues, transducer force, and intra- and inter-observer variability. Numerous investigations have shown that it is readily possible to perform MRE in abdominal organs for detecting specific diseases, such as hepatic fibrosis and portal hypertension, which increase the stiffness of the liver and spleen. Other preliminary studies have demonstrated that it is possible to evaluate the mechanical properties of other abdominal structures, such as the pancreas and kidneys. These results will further motivate future studies incorporating MRE to study the normal and pathological mechanics and physiology of abdominal organs.

MRE has been shown to be capable of detecting alterations in the tissue mechanical properties of kidneys in vivo preclinical and clinical studies. In the kidney, shear wave elastography has been shown to be helpful in early noninvasive detection and management of patients with chronic kidney disease (CKD). Renal MRE is a promising noninvasive technique that might have pathologic and prognostic significance.

Acknowledgments

This publication is based upon work from COST Action PARENCHIMA, supported by European Cooperation in Science and Technology (COST). COST (www.cost.eu) is a funding agency for research and innovation networks. COST Actions help connect research initiatives across Europe and enable scientists to enrich their ideas by sharing them with their peers. This boosts their research, career, and innovation.

PARENCHIMA (renalMRI.org) is a community-driven Action in the COST program of the European Union, which unites more than 200 experts in renal MRI from 30 countries with the aim to improve the reproducibility and standardization of renal MRI biomarkers.

References

1. Yin M, Talwalkar JA, Glaser KJ, Manduca A, Grimm RC, Rossman PJ, Fidler JL, Ehman RL (2007) Assessment of hepatic fibrosis with magnetic resonance elastography. *Clin Gastroenterol Hepatol* 5(10):1207–1213.e1202. <https://doi.org/10.1016/j.cgh.2007.06.012>
2. Yin M, Woollard J, Wang X, Torres VE, Harris PC, Ward CJ, Glaser KJ, Manduca A, Ehman RL (2007) Quantitative assessment of hepatic fibrosis in an animal model with magnetic resonance elastography. *Magn Reson Med* 58(2):346–353. <https://doi.org/10.1002/mrm.21286>
3. Xanthakos SA, Podberesky DJ, Serai SD, Miles L, King EC, Balistreri WF, Kohli R (2014) Use of magnetic resonance elastography to assess hepatic fibrosis in children with chronic liver disease. *J Pediatr* 164(1):186–188. <https://doi.org/10.1016/j.jpeds.2013.07.050>

4. Muthupillai R, Ehman RL (1996) Magnetic resonance elastography. *Nat Med* 2 (5):601–603
5. Serai SD, Towbin AJ, Podberesky DJ (2012) Pediatric liver MR elastography. *Dig Dis Sci* 57 (10):2713–2719. <https://doi.org/10.1007/s10620-012-2196-2>
6. Fung YC (1993) Biomechanics mechanical properties of living tissues. Springer, New York, NY
7. Papazoglou S, Hirsch S, Braun J, Sack I (2012) Multifrequency inversion in magnetic resonance elastography. *Phys Med Biol* 57 (8):2329–2346. <https://doi.org/10.1088/0031-9155/57/8/2329>
8. Serai SD, Dillman JR, Trout AT (2017) Spin-echo echo-planar imaging MR elastography versus gradient-echo MR elastography for assessment of liver stiffness in children and young adults suspected of having liver disease. *Radiology* 282(3):761–770. <https://doi.org/10.1148/radiol.2016160589>
9. Calle-Toro JS, Serai SD, Hartung EA, Goldberg DJ, Bolster BD Jr, Darge K, Anupindi SA (2019) Magnetic resonance elastography SE-EPI vs GRE sequences at 3T in a pediatric population with liver disease. *Abdom Radiol*. <https://doi.org/10.1007/s00261-018-1884-6>
10. Serai SD, Obuchowski NA, Venkatesh SK, Sirlin CB, Miller FH, Ashton E, Cole PE, Ehman RL (2017) Repeatability of MR elastography of liver: a meta-analysis. *Radiology* 285 (1):92–100. <https://doi.org/10.1148/radiol.2017161398>
11. Loomba R, Cui J, Wolfson T, Haufe W, Hooker J, Szeverenyi N, Ang B, Bhatt A, Wang K, Aryafar H, Behling C, Valasek MA, Lin GY, Gamst A, Brenner DA, Yin M, Glaser KJ, Ehman RL, Sirlin CB (2016) Novel 3D magnetic resonance elastography for the non-invasive diagnosis of advanced fibrosis in NAFLD: a prospective study. *Am J Gastroenterol* 111(7):986–994. <https://doi.org/10.1038/ajg.2016.65>
12. Serai SD, Abu-El-Haija M, Trout AT (2019) 3D MR elastography of the pancreas in children. *Abdom Radiol*. <https://doi.org/10.1007/s00261-019-01903-w>
13. Mohamed AA, Elbedewy TA, El-Serafy M, El-Toukhy N, Ahmed W, Ali El Din Z (2015) Hepatitis C virus: a global view. *World J Hepatol* 7(26):2676–2680. <https://doi.org/10.4254/wjh.v7.i26.2676>
14. Ratziu V, Charlotte F, Heurtier A, Gombert S, Giral P, Bruckert E, Grimaldi A, Capron F, Poynard T (2005) Sampling variability of liver biopsy in nonalcoholic fatty liver disease. *Gastroenterology* 128(7):1898–1906
15. Regev A, Berho M, Jeffers LJ, Milikowski C, Molina EG, Pyrsopoulos NT, Feng ZZ, Reddy KR, Schiff ER (2002) Sampling error and intraobserver variation in liver biopsy in patients with chronic HCV infection. *Am J Gastroenterol* 97(10):2614–2618. <https://doi.org/10.1111/j.1572-0241.2002.06038.x>
16. Venkatesh SK, Ehman RL (2014) Magnetic resonance elastography of liver. *Magn Reson Imaging Clin N Am* 22(3):433–446. <https://doi.org/10.1016/j.mric.2014.05.001>
17. Trout AT, Serai S, Mahley AD, Wang H, Zhang Y, Zhang B, Dillman JR (2016) Liver stiffness measurements with MR elastography: agreement and repeatability across imaging systems, field strengths, and pulse sequences. *Radiology* 281(3):793–804. <https://doi.org/10.1148/radiol.2016160209>
18. Yin M, Glaser KJ, Talwalkar JA, Chen J, Manduca A, Ehman RL (2016) Hepatic MR elastography: clinical performance in a series of 1377 consecutive examinations. *Radiology* 278(1):114–124. <https://doi.org/10.1148/radiol.2015142141>
19. Pepin KM, McGee KP (2018) Quantifying tumor stiffness with magnetic resonance elastography: the role of mechanical properties for detection, characterization, and treatment stratification in oncology. *Top Magn Reson Imaging* 27(5):353–362. <https://doi.org/10.1097/rmr.0000000000000181>
20. Venkatesh SK, Yin M, Glockner JF, Takahashi N, Araoz PA, Talwalkar JA, Ehman RL (2008) MR elastography of liver tumors: preliminary results. *AJR Am J Roentgenol* 190 (6):1534–1540. <https://doi.org/10.2214/ajr.07.3123>
21. Garteiser P, Doblaz S, Daire JL, Wagner M, Leitao H, Vilgrain V, Sinkus R, Van Beers BE (2012) MR elastography of liver tumours: value of viscoelastic properties for tumour characterisation. *Eur Radiol* 22 (10):2169–2177. <https://doi.org/10.1007/s00330-012-2474-6>
22. Talwalkar JA, Yin M, Venkatesh S, Rossman PJ, Grimm RC, Manduca A, Romano A, Kamath PS, Ehman RL (2009) Feasibility of in vivo MR elastographic splenic stiffness measurements in the assessment of portal hypertension. *AJR Am J Roentgenol* 193(1):122–127. <https://doi.org/10.2214/AJR.07.3504>
23. Yin M, Chen J, Glaser KJ, Talwalkar JA, Ehman RL (2009) Abdominal magnetic resonance elastography. *Top Magn Reson Imaging* 20 (2):79–87. <https://doi.org/10.1097/RMR.0b013e3181c4737e>
24. Hartung EA, Wen J, Poznick L, Furth SL, Darge K (2019) Ultrasound elastography to

- quantify liver disease severity in autosomal recessive polycystic kidney disease. *J Pediatrics* 209:107–115.e105. <https://doi.org/10.1016/j.jpeds.2019.01.055>
25. Nangaku M (2004) Mechanisms of tubulointerstitial injury in the kidney: final common pathways to end-stage renal failure. *Intern Med* 43(1):9–17. <https://doi.org/10.2169/internalmedicine.43.9>
 26. Hodgkins KS, Schnaper HW (2012) Tubulointerstitial injury and the progression of chronic kidney disease. *Pediatr Nephrol* 27(6):901–909. <https://doi.org/10.1007/s00467-011-1992-9>
 27. Alukal JJ, Thuluvath PJ (2019) Reversal of NASH fibrosis with pharmacotherapy. *Hepatol Int* 13(5):534–545. <https://doi.org/10.1007/s12072-019-09970-3>
 28. Ismail MH, Pinzani M (2009) Reversal of liver fibrosis. *Saudi J Gastroenterol* 15(1):72–79. <https://doi.org/10.4103/1319-3767.45072>
 29. Schuppan D, Ashfaq-Khan M, Yang AT, Kim YO (2018) Liver fibrosis: direct antifibrotic agents and targeted therapies. *Matrix Biol* 68–69:435–451. <https://doi.org/10.1016/j.matbio.2018.04.006>
 30. Tampe D, Zeisberg M (2014) Potential approaches to reverse or repair renal fibrosis. *Nat Rev Nephrol* 10(4):226–237. <https://doi.org/10.1038/nrneph.2014.14>
 31. Bledsoe G, Shen B, Yao Y, Zhang JJ, Chao L, Chao J (2006) Reversal of renal fibrosis, inflammation, and glomerular hypertrophy by kallikrein gene delivery. *Hum Gene Ther* 17(5):545–555. <https://doi.org/10.1089/hum.2006.17.545>
 32. Klinkhammer BM, Goldschmeding R, Floege J, Boor P (2017) Treatment of renal fibrosis—turning challenges into opportunities. *Adv Chronic Kidney Dis* 24(2):117–129. <https://doi.org/10.1053/j.ackd.2016.11.002>
 33. Lee SY, Kim SI, Choi ME (2015) Therapeutic targets for treating fibrotic kidney diseases. *Transl Res* 165(4):512–530. <https://doi.org/10.1016/j.trsl.2014.07.010>
 34. Menn-Josephy H, Lee CS, Nolin A, Christov M, Rybin DV, Weinberg JM, Henderson J, Bonegio R, Havasi A (2016) Renal interstitial fibrosis: an imperfect predictor of kidney disease progression in some patient cohorts. *Am J Nephrol* 44(4):289–299. <https://doi.org/10.1159/000449511>
 35. dos Santos EA, Li LP, Ji L, Prasad PV (2007) Early changes with diabetes in renal medullary hemodynamics as evaluated by fiberoptic probes and BOLD magnetic resonance imaging. *Investig Radiol* 42(3):157–162. <https://doi.org/10.1097/01.rli.0000252492.96709.36>
 36. Li LP, Halter S, Prasad PV (2008) Blood oxygen level-dependent MR imaging of the kidneys. *Magn Reson Imaging Clin N Am* 16(4):613–625. <https://doi.org/10.1016/j.mric.2008.07.008>
 37. Pruijm M, Mendichovszky IA, Liss P, Van der Niepen P, Textor SC, Lerman LO, Krediet CTP, Caroli A, Burnier M, Prasad PV (2018) Renal blood oxygenation level-dependent magnetic resonance imaging to measure renal tissue oxygenation: a statement paper and systematic review. *Nephrol Dial Transplant* 33(Suppl_2):ii22–ii28. <https://doi.org/10.1093/ndt/gfy243>
 38. Caroli A, Schneider M, Friedli I, Ljimini A, De Seigneux S, Boor P, Gullapudi L, Kazmi I, Mendichovszky IA, Notohamiprodo M, Selby NM, Thoeny HC, Grenier N, Vallee JP (2018) Diffusion-weighted magnetic resonance imaging to assess diffuse renal pathology: a systematic review and statement paper. *Nephrol Dial Transplant* 33(Suppl_2):ii29–ii40. <https://doi.org/10.1093/ndt/gfy163>
 39. Ljimini A, Caroli A, Laustsen C, Francis S, Mendichovszky IA, Bane O, Nery F, Sharma K, Pohlmann A, Dekkers IA, Vallee JP, Derlin K, Notohamiprodo M, Lim RP, Palmucci S, Serai SD, Periquito J, Wang ZJ, Froeling M, Thoeny HC, Prasad P, Schneider M, Niendorf T, Pullens P, Sourbron S, Sigmund EE (2019) Consensus-based technical recommendations for clinical translation of renal diffusion-weighted MRI. *MAGMA*. <https://doi.org/10.1007/s10334-019-00790-y>
 40. Mansour SG, Puthumana J, Coca SG, Gentry M, Parikh CR (2017) Biomarkers for the detection of renal fibrosis and prediction of renal outcomes: a systematic review. *BMC Nephrol* 18(1):72. <https://doi.org/10.1186/s12882-017-0490-0>
 41. Serai SD, Trout AT, Miethke A, Diaz E, Xanthakos SA, Dillman JR (2018) Putting it all together: established and emerging MRI techniques for detecting and measuring liver fibrosis. *Pediatr Radiol* 48(9):1256–1272. <https://doi.org/10.1007/s00247-018-4083-2>
 42. Serai SD, Trout AT, Sirlin CB (2017) Elastography to assess the stage of liver fibrosis in children: concepts, opportunities, and challenges. *Clin Liver Dis* 9(1):5–10. <https://doi.org/10.1002/cld.607>

43. Sigrist RMS, Liau J, Kaffas AE, Chammas MC, Willmann JK (2017) Ultrasound elastography: review of techniques and clinical applications. *Theranostics* 7(5):1303–1329. <https://doi.org/10.7150/thno.18650>
44. Menziloglu MS, Duymus M, Citil S, Avcu S, Gungor G, Sahin T, Boysan SN, Altunoren O, Sarica A (2015) Strain wave elastography for evaluation of renal parenchyma in chronic kidney disease. *Br J Radiol* 88(1050):20140714. <https://doi.org/10.1259/bjr.20140714>
45. Wang L, Xia P, Lv K, Han J, Dai Q, Li XM, Chen LM, Jiang YX (2014) Assessment of renal tissue elasticity by acoustic radiation force impulse quantification with histopathological correlation: preliminary experience in chronic kidney disease. *Eur Radiol* 24(7):1694–1699. <https://doi.org/10.1007/s00330-014-3162-5>
46. Bob F, Bota S, Sporea I, Sirlu R, Popescu A, Schiller A (2015) Relationship between the estimated glomerular filtration rate and kidney shear wave speed values assessed by acoustic radiation force impulse elastography: a pilot study. *J Ultrasound Med* 34(4):649–654. <https://doi.org/10.7863/ultra.34.4.649>
47. Bota S, Herkner H, Sporea I, Salzl P, Sirlu R, Neghina AM, Peck-Radosavljevic M (2013) Meta-analysis: ARFI elastography versus transient elastography for the evaluation of liver fibrosis. *Liver Int* 33(8):1138–1147. <https://doi.org/10.1111/liv.12240>
48. Lee CU, Glockner JF, Glaser KJ, Yin M, Chen J, Kawashima A, Kim B, Kremers WK, Ehman RL, Gloor JM (2012) MR elastography in renal transplant patients and correlation with renal allograft biopsy: a feasibility study. *Acad Radiol* 19(7):834–841. <https://doi.org/10.1016/j.acra.2012.03.003>
49. Zhang X, Zhu X, Ferguson CM, Jiang K, Burningham T, Lerman A, Lerman LO (2018) Magnetic resonance elastography can monitor changes in medullary stiffness in response to treatment in the swine ischemic kidney. *MAGMA* 31(3):375–382. <https://doi.org/10.1007/s10334-017-0671-7>
50. Grenier N, Poulain S, Lepreux S, Gennisson JL, Dallaudiere B, Lebras Y, Bavu E, Servais A, Meas-Yedid V, Piccoli M, Bachelet T, Tanter M, Merville P, Couzi L (2012) Quantitative elastography of renal transplants using supersonic shear imaging: a pilot study. *Eur Radiol* 22(10):2138–2146. <https://doi.org/10.1007/s00330-012-2471-9>
51. Orlicchio A, Chegai F, Del Giudice C, Anselmo A, Iaria G, Palmieri G, Di Caprera E, Tosti D, Costanzo E, Tisone G, Simonetti G (2014) Kidney transplant: usefulness of real-time elastography (RTE) in the diagnosis of graft interstitial fibrosis. *Ultrasound Med Biol* 40(11):2564–2572. <https://doi.org/10.1016/j.ultrasmedbio.2014.06.002>
52. Itokawa F, Itoi T, Sofuni A, Kurihara T, Tsuchiya T, Ishii K, Tsuji S, Ikeuchi N, Umeda J, Tanaka R, Yokoyama N, Moriyasu F, Kasuya K, Nagao T, Kamisawa T, Tsuchida A (2011) EUS elastography combined with the strain ratio of tissue elasticity for diagnosis of solid pancreatic masses. *J Gastroenterol* 46(6):843–853. <https://doi.org/10.1007/s00535-011-0399-5>
53. Erkan M, Hausmann S, Michalski CW, Schlitter AM, Fingerle AA, Dobritz M, Friess H, Kleeff J (2012) How fibrosis influences imaging and surgical decisions in pancreatic cancer. *Front Physiol* 3:389. <https://doi.org/10.3389/fphys.2012.00389>
54. An H, Shi Y, Guo Q, Liu Y (2016) Test-retest reliability of 3D EPI MR elastography of the pancreas. *Clin Radiol* 71(10):1068.e1012–1068.e1012. <https://doi.org/10.1016/j.crad.2016.03.014>
55. Wang M, Gao F, Wang X, Liu Y, Ji R, Cang L, Shi Y (2018) Magnetic resonance elastography and T1 mapping for early diagnosis and classification of chronic pancreatitis. *J Magn Reson Imaging*. <https://doi.org/10.1002/jmri.26008>
56. Barton MB, Harris R, Fletcher SW (1999) The rational clinical examination. Does this patient have breast cancer? The screening clinical breast examination: should it be done? How? *JAMA* 282(13):1270–1280. <https://doi.org/10.1001/jama.282.13.1270>
57. Lorenzen J, Sinkus R, Lorenzen M, Dargatz M, Leussler C, Roschmann P, Adam G (2002) MR elastography of the breast: preliminary clinical results. *Rofo* 174(7):830–834. <https://doi.org/10.1055/s-2002-32690>
58. McKnight AL, Kugel JL, Rossman PJ, Manduca A, Hartmann LC, Ehman RL (2002) MR elastography of breast cancer: preliminary results. *AJR Am J Roentgenol* 178(6):1411–1417. <https://doi.org/10.2214/ajr.178.6.1781411>
59. Kim HK, Lindquist DM, Serai SD, Mariappan YK, Wang LL, Merrow AC, McGee KP, Ehman RL, Laor T (2013) Magnetic resonance imaging of pediatric muscular disorders: recent advances and clinical applications. *Radiol Clin N Am* 51(4):721–742. <https://doi.org/10.1016/j.rcl.2013.03.002>
60. Basford JR, Jenkin TR, An KN, Ehman RL, Heers G, Kaufman KR (2002) Evaluation of healthy and diseased muscle with magnetic resonance elastography. *Arch Phys Med Rehabil*

- 83(11):1530–1536. <https://doi.org/10.1053/apmr.2002.35472>
61. Pichiecchio A, Alessandrino F, Bortolotto C, Cerica A, Rosti C, Raciti MV, Rossi M, Berardinelli A, Baranello G, Bastianello S, Calliada F (2018) Muscle ultrasound elastography and MRI in preschool children with Duchenne muscular dystrophy. *Neuromuscul Dis* 28 (6):476–483. <https://doi.org/10.1016/j.nmd.2018.02.007>
 62. Buechter M, Manka P, Theysohn JM, Reinboldt M, Canbay A, Kahraman A (2018) Spleen stiffness is positively correlated with HVPg and decreases significantly after TIPS implantation. *Dig Liver Dis* 50(1):54–60. <https://doi.org/10.1016/j.dld.2017.09.138>
 63. Song J, Huang J, Huang H, Liu S, Luo Y (2018) Performance of spleen stiffness measurement in prediction of clinical significant portal hypertension: a meta-analysis. *Clin Res Hepatol Gastroenterol* 42(3):216–226. <https://doi.org/10.1016/j.clinre.2017.11.002>
 64. Yin M, Kolipaka A, Warner L, Talwalkar JA, Manduca A, Ehman RL (2010) Influence of perfusion on tissue stiffness assessed with MR elastography. *Proc Int Soc Magn Reson Med* 18:256
 65. Yin M, Talwalkar JA, Glaser KJ, Venkatesh SK, Chen J, Manduca A, Ehman RL (2011) Dynamic postprandial hepatic stiffness augmentation assessed with MR elastography in patients with chronic liver disease. *AJR Am J Roentgenol* 197(1):64–70. <https://doi.org/10.2214/AJR.10.5989>
 66. Clark WF, Sontrop JM, Moist L, Huang SH (2015) Increasing water intake in chronic kidney disease: why? Safe? Possible? *Ann Nutr Metab* 66(Suppl 3):18–21. <https://doi.org/10.1159/000381241>
 67. Gandhi D, Kalra P, Raterman B, Mo X, Dong H, Kolipaka A (2019) Magnetic resonance elastography-derived stiffness of the kidneys and its correlation with water perfusion. *NMR Biomed* 33:e4237. <https://doi.org/10.1002/nbm.4237>
 68. Warner L, Yin M, Glaser KJ, Woollard JA, Carrascal CA, Korsmo MJ, Crane JA, Ehman RL, Lerman LO (2011) Noninvasive in vivo assessment of renal tissue elasticity during graded renal ischemia using MR elastography. *Investig Radiol* 46(8):509–514. <https://doi.org/10.1097/RLI.0b013e3182183a95>
 69. Ramachandran P, Iredale JP (2009) Reversibility of liver fibrosis. *Ann Hepatol* 8(4):283–291
 70. Campana L, Iredale JP (2017) Regression of liver fibrosis. *Semin Liver Dis* 37(1):1–10. <https://doi.org/10.1055/s-0036-1597816>
 71. Dong H, Mazumder R, Illapani VSP, Mo X, White RD, Kolipaka A (2017) In vivo quantification of aortic stiffness using MR elastography in hypertensive porcine model. *Magn Reson Med* 78(6):2315–2321. <https://doi.org/10.1002/mrm.26601>
 72. Morin CE, Dillman JR, Serai SD, Trout AT, Tkach JA, Wang H (2018) Comparison of Standard Breath-Held, Free-Breathing, and Compressed Sensing 2D Gradient-Recalled Echo MR Elastography Techniques for Evaluating Liver Stiffness. *AJR American journal of roentgenology*:1–9. doi:<https://doi.org/10.2214/ajr.18.19761>
 73. Liu X, Li N, Xu T, Sun F, Li R, Gao Q, Chen L, Wen C (2017) Effect of renal perfusion and structural heterogeneity on shear wave elastography of the kidney: an in vivo and ex vivo study. *BMC Nephrol* 18(1):265. <https://doi.org/10.1186/s12882-017-0679-2>

Open Access This chapter is licensed under the terms of the Creative Commons Attribution 4.0 International License (<http://creativecommons.org/licenses/by/4.0/>), which permits use, sharing, adaptation, distribution and reproduction in any medium or format, as long as you give appropriate credit to the original author(s) and the source, provide a link to the Creative Commons license and indicate if changes were made.

The images or other third party material in this chapter are included in the chapter's Creative Commons license, unless indicated otherwise in a credit line to the material. If material is not included in the chapter's Creative Commons license and your intended use is not permitted by statutory regulation or exceeds the permitted use, you will need to obtain permission directly from the copyright holder.

